atmosphere

MDPI

Article

# Source Apportionment of Volatile Organic Compounds (VOCs) during Ozone Polluted Days in Hangzhou, China

**Lixia Han [1], Linghong Chen [1,*], Kangwei Li [1,2], Zhier Bao [1], Yanyun Zhao [1], Xin Zhang [1], Merched Azzi [2] and Kefa Cen [1]**

[1] State Key Laboratory of Clean Energy Utilization, Zhejiang University, Hangzhou 310027, China; hanlxzju@foxmail.com (L.H.); likangweizju@foxmail.com (K.L.); baoxiaotu@foxmail.com (Z.B.); 21860069@zju.edu.cn (Y.Z.); 21860063@zju.edu.cn (X.Z.); kfcen@zju.edu.cn (K.C.)

[2] CSIRO Energy, PO Box 52, North Ryde, NSW 1670, Australia; Merched.Azzi@csiro.au

* Correspondence: chenlh@zju.edu.cn

Received: 07 November; Accepted: 02 December 2019; Published: 5 December 2019

**Abstract:** A field sampling campaign of volatile organic compounds (VOCs) was conducted during ozone polluted days at three sites of botanic gardens (HP), industrial areas (XS), and traffic residential mixed areas (ZH) in Hangzhou. The sampling was performed using stainless steel canisters from 6:00 to 20:00 synchronously with a time interval of 2 h on 17 May, 26 June, 20 July, 24 August, and 26 September 2018. A total of 107 species of VOCs for each sample were quantified using two standard gases with a pre-concentrator coupled by GC/MS. The Positive Matrix Factorization (PMF) model was used to identify the major VOC sources and assess their contribution to VOC concentrations. The effects of VOCs on $O_3$ formation were investigated, based on propylene-equivalent concentrations (Prop-E), ozone formation potential (OFP), and Smog Production Model (SPM). It was found that the concentration of ozone during the sampling days tended to be highest in the downwind area while the concentrations of VOCs and $NO_2$ in HP were rather low. The most reactive species were isoprene, ethylene, m-xylene, toluene, and propylene. The average total VOC volume mixing ratios in HP, XS, and ZH were 32.00, 36.63, and 50.34 ppbv, respectively. Bimodal profiles of propane and n-butane were exhibited in ZH while unimodal diurnal variation of isoprene was performed in HP. Liquefied petroleum gas/natural gas (LPG/NG) usage, aged background, and secondary source were identified as the major contributors to total VOCs in Hangzhou, accounting for 19.65%, 15.53%, and 18.93%, respectively.

**Keywords:** VOCs; spatial and temporal characteristics; source apportionment; $O_3$ formation

## 1. Introduction

Over the last few years, high level ozone ($O_3$) has become a critical air pollution issue during summer in China, especially in megacities and fast-developing city clusters [1–5]. It was well known that volatile organic compounds (VOCs) are the key precursors of $O_3$ and secondary organic aerosols (SOA) [6,7]. Due to the complex chemical mechanisms and diurnal variation of VOCs, there is a high nonlinear relationship between $O_3$ and its precursors [8]. Jin et al. showed that the cities in China were becoming increasingly VOC-limited [9]. Due to the diverse VOCs species and activities, it is necessary to understand their roles in $O_3$ formation for making appropriate control strategies.

Ozone has been recognized as the major photochemical smog oxidant in several megacities all over China [10–12]. Hangzhou, capital of Zhejiang province, is one of the largest cities in east coastal areas of China. With the rapid development of the economy and increase of population, Hangzhou

has suffered from severe atmospheric pollution in recent years, and the maximum 1 h $O_3$ mass concentration reached 327 μg/m$^3$ in 2016. $O_3$ pollution events occurred mainly under a VOC-limited or transitional regime in Hangzhou [13]. Understanding the role of key VOC species and their associated spatial and temporal distribution in the formation of photochemical smog episodes in Hangzhou, becomes a critical topic to be understood and resolved.

A vital purpose of ambient VOCs measurements is to identify their sources and their potential contributions in the formation of ozone and other photochemical smog oxidants. The Positive Matrix Factorization (PMF) method is a multivariate statistical analysis that was comprehensively described by Paatero in 1993 [14,15]. As a receptor model, the sources of VOCs can be identified and quantified with the use of PMF when numerous samples are obtained while complete emission source profiles are not available. Furthermore, PMF can be used to detect low value data and makes sure all the results are positive values. However, the name of factors mostly depends on the experience of analyzers to explain the intrinsic characteristics of different sources, which causes the explanations to vary from study to study. Even different tracers were chosen in the same factor name, like the description of LPG profiles in several papers [16–18].

In order to understand characteristics and sources of VOC compositions, we performed a simultaneous sampling campaign for five selected days with high $O_3$ levels (from May to September 2018) at three functional zones in Hangzhou. A total of 107 VOC species were quantified by laboratory analysis using a pre-concentrator with gas chromatography/mass spectrometry (GC/MS). General information about the sampling sites, instruments, and analysis methods was documented. Then the spatial and temporal variation in VOCs and relevant pollutants at the three sites were characterized. The PMF model was used to identify the major VOC sources and assess their contribution to VOC concentrations. The accuracy of the source apportionment results was examined by the comparison between PMF factors and measured source profiles. Finally, the effects of VOCs on $O_3$ formation were investigated, based on propylene-equivalent concentrations (Prop-E), ozone formation potential (OFP), and Smog Production Model (SPM).

## 2. Methods

### *2.1. Ambient VOCs and Source Profiles Sampling*

Hangzhou is located in the south of Yangtze River Delta (YRD) and lies on downstream of the Qiantang River (Figure 1). There is a West Lake and high green coverage rate in the south–west. In the eastern suburb of the city, two economic development zones, called Xiasha and Dajiangdong, are full of pollution-intensive industries. With the high population density and rapid economic growth, the number of motor vehicles increased from 0.39 million in 2000 to 2.79 million in 2017.

To determine the characteristics and source contributions of ambient VOCs in Hangzhou, three representative functional zones were chosen as sampling sites (shown in Figure 1): Huapu location (HP, 30.25° N, 120.12° E), as a botanic garden, is situated on viewing platform (≈20 m above ground) of West Lake Scenic Area, and the main surrounding emission sources are plants. Xiasha location (XS, 30.30° N, 120.34° E) is located on the roof of a hotel in industrial parks (21.5 km east of HP). This district is surrounded by major industries, such as chemical fiber, paint manufacturing, and electronic companies. Zhaohui location (ZH, 30.23° N, 120.16° E) is on the roof of a building in traffic and residential mixed areas (4.9 km northeast of HP). Except for heavy traffic emissions, there are large housing estates and hospitals in the area within a 1 km radius. The three sampling sites in different functional zones can represent the pollution situation of Hangzhou, and they are 365, 550, and 700 m apart from nearest monitoring air quality stations, respectively. The site location information and $O_3$ exceedance are shown in Table S1.

An ozone exceedance day was defined where the maximum daily 1 h $O_3$ concentration exceeded 200 μg/m$^3$ or the maximum daily average 8 h $O_3$ concentration exceeded 160 μg/m$^3$ (Chinese Ambient Air Quality Grade II Standard GB3095-2012). Since $O_3$ exceedance events in Hangzhou mainly occur in summer, sunny and hot days were chosen in every month from May to September to collect air samples [19]. In order to cover morning-evening rush hours, the sampling of VOCs was performed

from 6:00 to 20:00 at a time interval of 2 h on 17 May, 26 June, 20 July, 24 August, and 26 September 2018. A total of 120 valid samples were obtained, and the hourly meteorological conditions as well as relevant pollutants were collected from air quality stations including temperature, solar radiation, wind speed, wind direction, concentrations of NO, $NO_2$, $O_3$, CO, $SO_2$, $PM_{2.5}$, and $PM_{10}$.

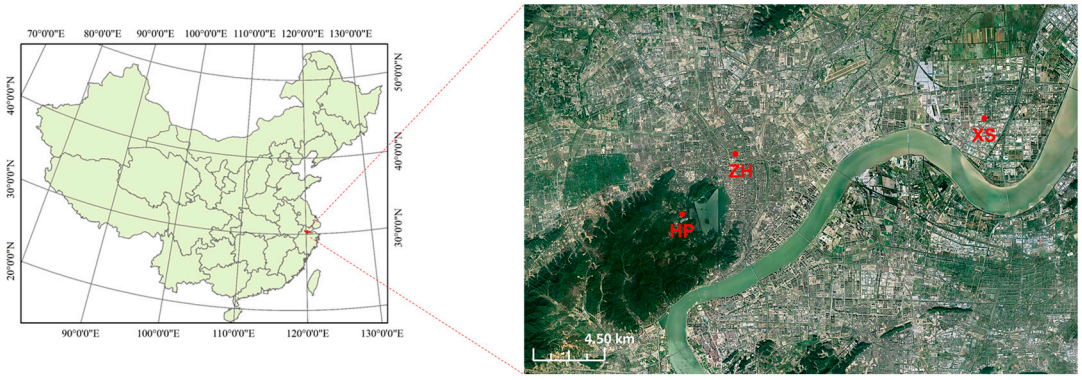


**Figure 1.** The location of Hangzhou in China (top left corner) and geographical distribution of three sampling sites.

Besides ambient VOCs sampling, source profiles of primary emission were sampled and established to examine the accuracy of the source apportionment results. Samples of solvent utilization were collected from production workshop in a paint factory. Biomass burning was collected from combustion in the laboratory. Additionally, vehicle exhaust was collected from a vehicle platform test station. The detailed information is shown in Table S2.

### *2.2. Analysis of VOC Samples*

Samples were collected using 3.2 L silica SUMMA canisters (Entech Instrument, Inc., Simi Valley, CA, USA), which were pre-cleaned with high-purity nitrogen and vacuumed to 20 Psi [20]. Ambient air was taken at a flow rate of 120 mL/min through a constant flow sampler (CS1200E, Entech Instrument, Inc., Simi Valley, CA, USA). After 30 min, canisters were pressurized to atmospheric pressure and valves were closed. All the samples were sent to laboratory for analysis within 7 days after collection.

Measurements of VOCs were made using a pre-concentrator followed by a gas chromatography/mass spectrometry (GC/MS). A 400 mL sample was extracted and concentrated in a cryogenic pre-concentrator (7200, Entech Instrument, Inc., Simi Valley, CA, USA), and a three-stage cold trap was used to remove the water, carbon dioxide, nitrogen, and oxygen in samples. Then VOCs were transferred into the GC/MS (7890B/5977A, Agilent Technologies, Inc., Santa Clara, CA, USA). A DB-5 ms capillary column (60 m × 320 μm × 1 μm) coupled with quadrupole mass spectrometer detector (35–300 u) was used for qualification and quantification. The GC column oven was programmed at 35 °C for 5 min initially, increasing to 120 °C at 5 °C/min, then immediately increasing to 220 °C at 10 °C/min and holding for 3 min. The entire duration of the processing was about 56 min.

The species of VOCs were qualified using two standard gases: PAMS and TO-15 that were recommended by US EPA. PAMS was a mixture of 55 nonmethane hydrocarbons (NMHCs) that primarily contributed to atmospheric photochemical reactions, and TO-15 was 65 nonpolar or weakly polar toxic VOCs. After removing the overlap species between the two standard gases, the 107 VOCs were measured, including 29 alkanes, 11 alkenes, one alkyne, 35 halocarbons, 18 aromatics, 12 oxygenated volatile organic compounds (OVOCs), and $CS_2$. Calibration curves were made by the standard gas mixtures at five concentrations, ranging from 1 to 20 ppbv. The correlation coefficients of each curve were greater than 0.9, and the method detection limit (MDL) of individual species ranged from 0.002 to 0.09 ppbv.

### *2.3. Positive Matrix Factorization (PMF)*

Source apportionment of ambient VOCs was performed by the PMF 5.0 model. The fundamental equation is presented as follows:

$$x_{ij} = \sum_{k=1}^{p} g_{ik} f_{kj} + e_{ij}, \quad (1)$$

where $x_{ij}$ is the concentration of $j$th species in $i$th sample, $g_{ik}$ is the relative contribution of $k$th factor to $i$th sample, $f_{kj}$ is the $j$th species fraction in $k$th factor profiles, $e_{ij}$ is the residual for $j$th species in $i$th sample [14].

The objective function $Q$ needs to be minimized in the calculation of PMF model, and the $Q$ equation is presented as follows [21]:

$$Q = \sum_{i=1}^{n} \sum_{j=1}^{m} \left( \frac{e_{ij}}{u_{ij}} \right)^2, \quad (2)$$

where $u_{ij}$ is the uncertainty of $j$th species in $i$th sample. At the constraint condition of $g_{ik} \geq 0$ and $f_{kj} \geq 0$, the minimum $Q$ value is worked out by iterative convergence. Eventually, factor numbers, contribution matrix, and factor profiles matrices are resolved [22].

Two input files are required in the PMF 5.0, one with mass concentrations of observed sampling species and the other with uncertainty. The stability and accuracy of results are estimated by $Q$(true)/$Q$(expected), residual distribution, coefficient of determination, and explanation of factor profiles. Besides, these strict quality standards are the basis of reasonable source apportionment.

In PMF analysis, volume mixing ratio (unit in ppbv) is convert to mass concentration (unit in μg/m$^3$) because of the comparison between resolved factors and VOC source profiles. The formula is presented as follows:

$$C(\mu g/m^3) = c(\text{ppbv}) \times \frac{M \times 273.15}{22.4 \times (273.15 + T)}, \quad (3)$$

where $M$ is the molecular weight of the species, $T$ is the ambient temperature.

### *2.4. Photochemical Reactivity*

Generally, propylene-equivalent concentrations (Prop-E) and ozone formation potential (OFP) are used as indicators to evaluate the reactivity of VOCs. The principle of Prop-E is putting all VOC species on the same level to compare the reactivity with OH radical. The formula is presented as follows [23]:

$$\text{Prop-E}(j) = C_j \times [\text{VOC}]_j \times \frac{k_{\text{OH}}(j)}{k_{\text{OH}}(\text{C}_3\text{H}_6)}, \quad (4)$$

where $j$ is a species of VOC, $C_j$ represents its carbon atom number, $[\text{VOC}]_j$ represents its volume mixing ratio, $k_{\text{OH}}(j)$ and $k_{\text{OH}}(\text{C}_3\text{H}_6)$ represent the chemical reaction rate constant of species $j$ and propylene with OH radical [24].

We used the Prop-E method to evaluate the species activity in terms of the initial reaction rate of VOCs and OH, ignoring the reaction with peroxide and other radicals. On this basis, Cater et al. proposed a concept of OFP, which estimated the maximum VOCs contribution to $O_3$ formation synthetically. The specific calculation formula is as follows [25]:

$$\text{OFP} = [\text{VOC}]_j \times \text{MIR}_j, \quad (5)$$

where $\text{MIR}_j$ is the maximum incremental reactivity coefficient of $j$ species.

### *2.5. Smog Production Model*

The smog production model (SPM) was used to determine the $O_3$ photochemical regimes [26]. SP is defined by the sum of $O_3$ production and NOx consumption, according to the following two alternative equations [27]:

$$SP(t) = O_3(t) + DO_3(t) - O_3(0) + NO(i) - NO(t), \quad (6)$$

$$SP(t) = \beta\,[NOx(i) - NOx(t)]^{\alpha}, \quad (7)$$

where $O_3(t)$ is the $O_3$ concentration at time $t$, $DO_3(t)$ represents the accumulated deposition losses of ozone at time $t$, $O_3(0)$ is the background concentration of ambient $O_3$, with a value of 40 ppbv used in this study, NO($i$) is the input concentration of NO to the system from time 0 to $t$, NO($t$) is the NO concentration at time $t$, NOx($i$) is the input concentration of NOx to the system from time 0 to $t$, NOx($t$) is the NOx concentration at time $t$, $\alpha$ and $\beta$ is the parameters, with value of 2/3 and 19.

The maximum potential SP is defined as

$$SP_{max} = \beta[NOx(i)]^{\alpha}. \quad (8)$$

The extent of reaction $E(t) = SP(t)/SP_{max}$ is given by

$$E(t) = \frac{O_3(t) + DO_3(t) - O_3(0) + NO(i) - NO(t)}{\beta[NOx(i)]^{\alpha}}, \quad (9)$$

$$E(t) = \left[1 - \frac{NOx(t)}{NOx(i)}\right]^{\alpha}, \quad (10)$$

where $E(t)$ is estimated as the average of above two calculations (Equations (9) and (10)), and more details are presented by Li et al. [13].

## 3. Results and Discussion

### *3.1. Spatial-Temporal Characteristics of VOCs*

#### 3.1.1. Overall Meteorology and Pollutants

The $O_3$ exceedance in summer is not only closely related to precursors of VOCs and NOx, but also influenced by meteorological condition [28]. Figure 2 illustrates an overview of the temporal variations in the temperature, total solar radiation, wind speed, wind direction in Hangzhou, and the concentrations of $NO_2$, $O_3$ at the three sampling sites during the five sampling days. The temperature and solar radiation basically maintained the same level across the five days except for 26 September. Meanwhile, among the five days, the lowest $O_3$ level was observed on 26 September, because the temperature and radiation had a positive impact on the more biogenic emissions, chemical kinetic rates, and mechanism pathway for $O_3$ formation [29].

The concentration of $NO_2$ in HP was lower than in XS and ZH, because XS was affected by industrial emissions and ZH by vehicle exhausts. $O_3$ concentration was not closely related to pollutants emissions of three sites, and it depended on diffusion conditions. For example, the wind field was dominated by west and southwest wind on 17 May and 26 June, and the highest $O_3$ concentration appeared in XS which was in the downwind area. However, the wind came from the east on 20 July, which made HP in the downwind show the highest $O_3$ concentration. The prevailing wind direction was irregular on 24 August and north on 26 September, thus there was no obvious difference of downwind and $O_3$ concentration among the three sampling sites.

According to the ozone exceedance standard, the $O_3$ concentration exceeded in XS on 17 May, HP on 20 July, and three sites on 24 August. The diurnal variation of $O_3$ on 17 May and 24 August were chosen as two representative cases to be analyzed in detail. As shown in Figures 2 and S1, $O_3$ concentration was highest in 12:00–14:00 and kept consistent in the whole YRD on 17 May, indicating that $O_3$ peaks were the typical product of local photochemical reaction. This situation was different on 24 August: Figure 2d shows that there were two peaks of $O_3$ at the three sites, and the second peak

was at about 20:00. This was further illustrated by Figure S2 that the first peak at 14:00 was caused by photochemical reaction covering the whole YRD, and the second peak at 20:00 was transported from northeast, which coincided with $O_3$ spatial distribution and wind direction.

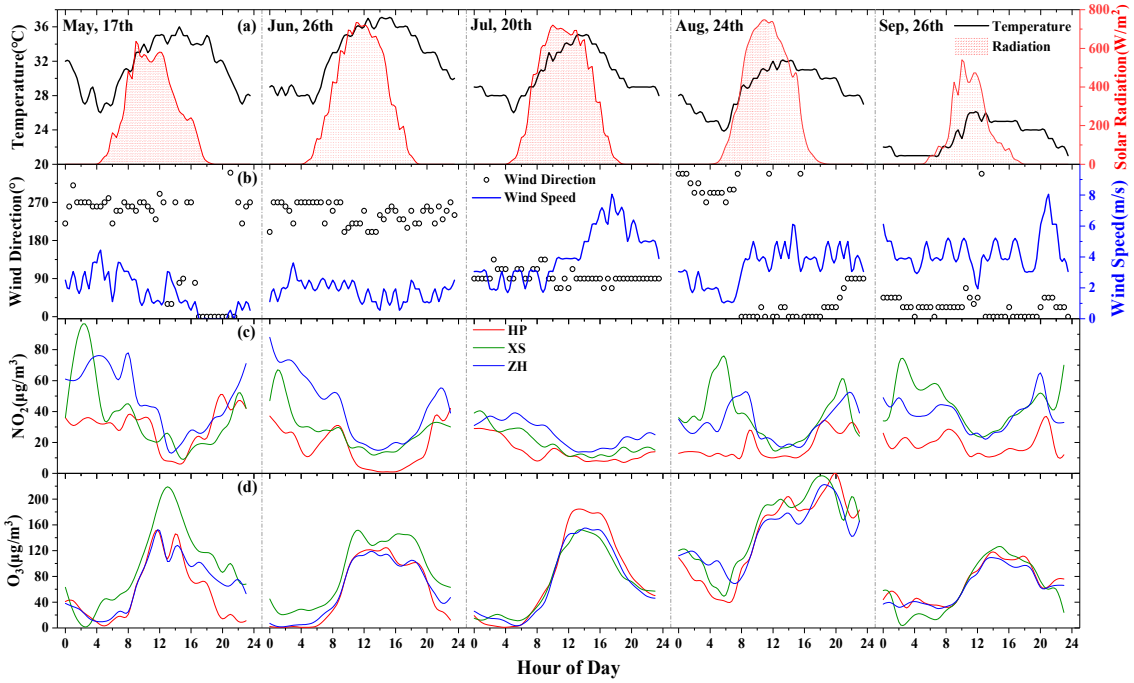


**Figure 2.** Time series of (**a**) temperature and solar radiation, (**b**) wind direction and wind speed in Hangzhou, (**c**) concentrations of $NO_2$ and (**d**) $O_3$ at the three sites during sampling days.

The average total VOC volume mixing ratios in HP, XS, and ZH were 32.00, 36.63, and 50.34 ppbv, respectively. Top 10 VOCs species in different groups (alkanes, alkenes, and alkynes, halocarbons, aromatics, OVOCs, and $CS_2$) are shown in Figure 3. As for alkanes, there was a significant similarity of display orders and concentrations between HP and XS, and C2–C5 alkanes were more abundant in ZH due to vehicle emissions. As for alkenes and alkynes, ethylene, isoprene, propylene, acetylene, and 1-butene were the major species at the three sites. Except these, concentrations of other species were extremely low. As for halocarbons, there was a similar display of orders and concentrations in HP and XS, and 1,2-dichloroethane were more abundant in ZH than the other two sites. As for aromatics, toluene were the most abundant species among the three sites. Moreover, the concentration of toluene was higher in XS and ZH than HP because of solvent usage and vehicle emissions. As for OVOCs and $CS_2$, acetone was the most abundant compound at the three sites (7.60–10.82 ppbv), accounting for about 20% among the 107 species. The high concentration of acetone in our research was similar to the previous studies in Beijing (8.00 ppbv), Guangzhou (6.41 ppbv), and the selected public places of Hangzhou (7.11 ppbv) [30–32].

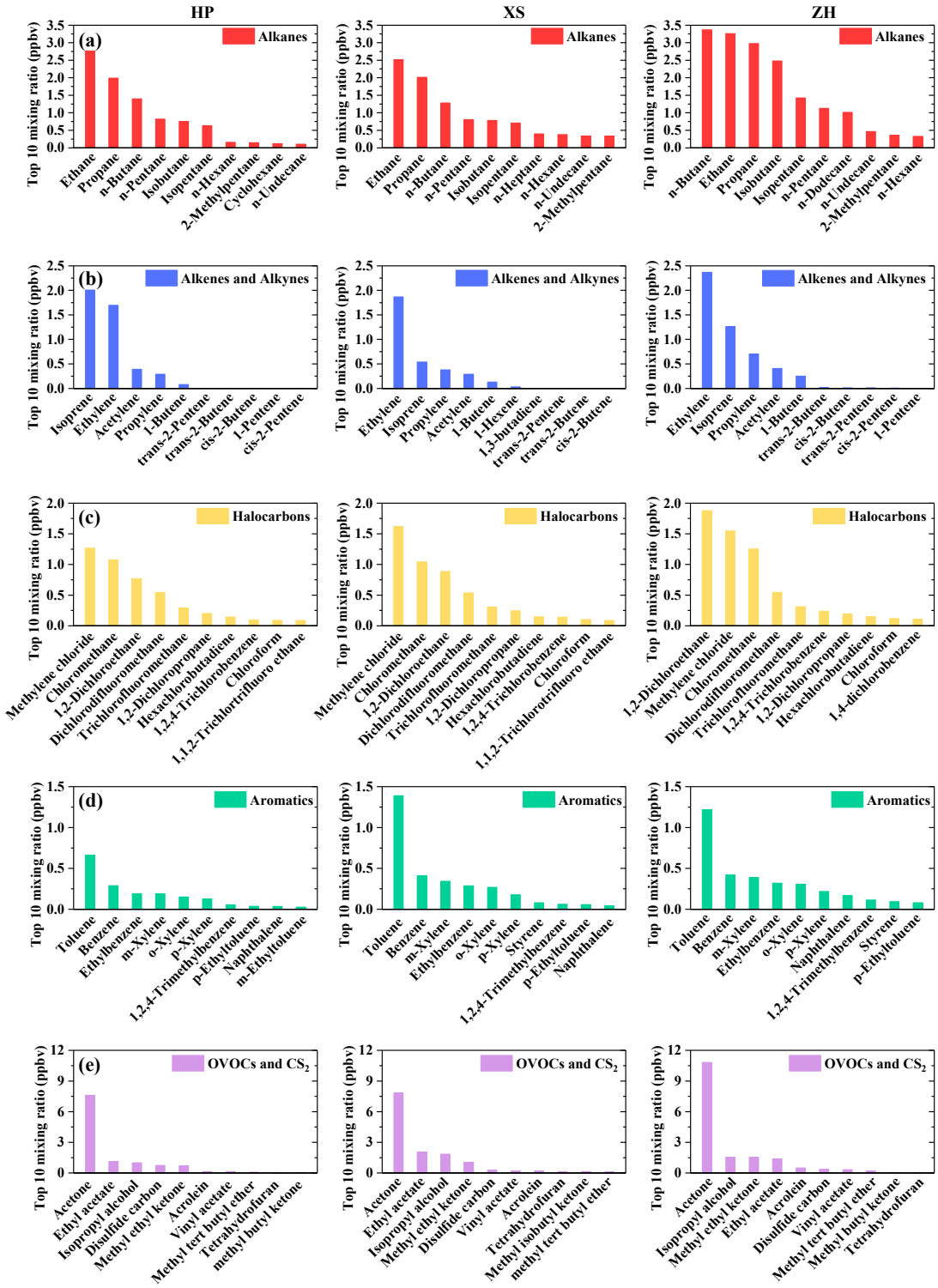


**Figure 3.** Top 10 mixing ratio of different volatile organic compound (VOC) groups ((**a**) alkanes, (**b**) alkenes and alkynes, (**c**) halocarbons, (**d**) aromatics, (**e**) oxygenated volatile organic compounds (OVOCs) and $CS_2$) at the three sites.

Table S3 shows the concentrations of main VOCs observed in other cities (Beijing, Shanghai, Guangzhou, and Wuhan) as well as Hangzhou [33–36]. The comparison indicated that concentrations of TVOCs in Hangzhou were similar to Shanghai and Wuhan, but much lower than Beijing and Guangzhou. Regarding each species, there were no definite rules to follow since human activities and energy structure may lead to the pollution status of VOCs [37].

There were 11 species in which more than 95% of sample concentrations were below the MDL. Their names are listed in Table S4, where alkanes and alkenes dominated. These species were few in the three different positional and functional areas, which represented that the emissions of them were very low in Hangzhou and the emission reductions could be left out at present.

#### 3.1.2. Diurnal Variation of VOCs

Figure S3 shows the diurnal variation of VOC concentrations and standard deviations in total VOCs and different groups (alkanes, alkenes and alkynes, halocarbons, aromatics, and OVOCs) at the three sampling sites. The mixing ratio of TVOCs, alkanes, and OVOCs in ZH were obviously greater than the rest of the sites. Mainly influenced by the vehicle exhaust, alkanes, aromatics, alkenes and alkynes of ZH exhibited bimodal profiles, which were consistent with the morning and evening rush hours (8:00 and 18:00–20:00). The morning peak was more distinct due to the accumulation of pollutants during the whole night. In XS sites, there was a U-shaped distribution of TVOCs and all groups: the concentrations reached highest at 6:00 or 20:00, lowest at noon, which had a relationship with the nearby industrial emission process, intensity of photolysis loss and diurnal variation of atmospheric boundary layer [38,39]. As a background site, lower concentrations and more steady variation of TVOCs, alkanes, halocarbons, aromatics, and OVOCs was shown in HP, though these groups fluctuated affected by diffusion of the surrounding pollutants. Isoprene, an indicator of biogenic emissions, was abundant in the scenic spots, making the concentrations of alkenes and alkynes in HP higher than XS.

Figure 4 shows the diurnal variations of some significant species, like ethane, propane, n-butane, ethylene, isoprene, chloromethane, 1,2-dichloroethane, toluene, and acetone in the three sampling sites. Ethane and ethylene exhibited similar diurnal patterns, which indicated that they might be from the same source. Propane and n-butane, tracers of vehicle exhaust, were much more abundant in ZH, and these two species exhibited bimodal profiles, which were consistent with the traffic flow. Isoprene was the indicator of biogenic emissions, and as expected its concentration was much higher in HP than XS and ZH during the day time. The unimodal distribution of isoprene was proportional to temperature and biogenic emission rates. Chloromethane and 1,2-dichloroethane were unreactive species with long lifespan, thus their concentrations were relatively steady. The diurnal variation of toluene in ZH was similar to HP because of the same emission sources and removal mechanisms. The concentration of acetone was relatively steady in XS due to the stable solvent usage. The concentration of acetone reached higher after 8:00 in HP and ZH, which indicated that acetone might be related to the production of photochemical reactivity in the two sites.

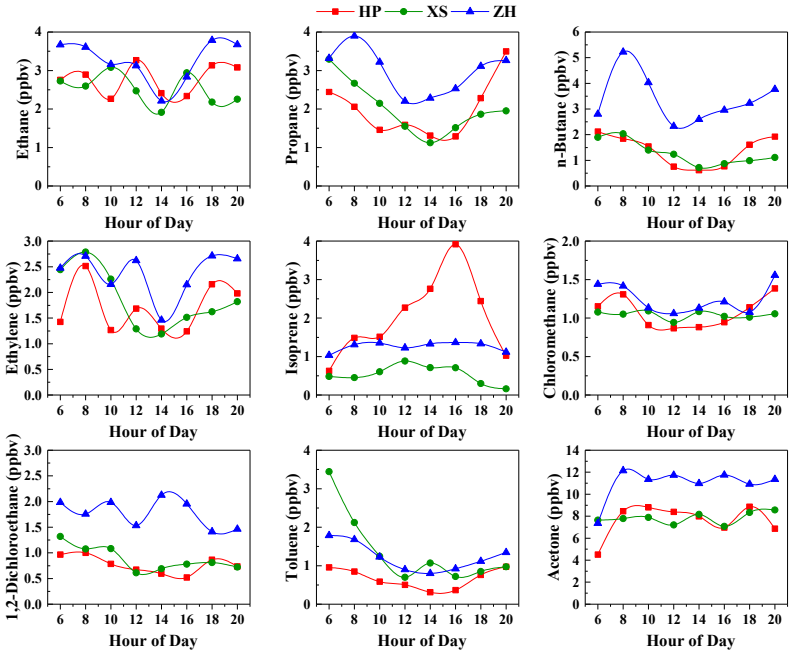


**Figure 4.** Diurnal variation of some significant species at the three sampling sites.

## 3.2. *Source Apportionment and Source Profiles of VOCs*

### 3.2.1. Source Profiles of PMF Resolved Factors

A total of 36 VOC species were chosen as input of the PMF model to explore the sources of observed VOCs, because they were the most abundant VOCs or the typical tracers of different emission sources. After a series of calculations, seven factors were classified as liquefied petroleum gas/natural gas (LPG/NG) usage, solvent utilization, biomass burning, vehicle exhaust, aged background, secondary source, and biogenic emission. Figure 5 presents the explained variation (EV) for all the factors, which indicated the importance of each factor to individual species. The name of factors was determined by the high contributions to tracers in a specific factor, as well as the comparison of species fraction between measured source profiles and PMF factors in Figure S4. The diurnal variation of seven sources are plotted in Figure 6, which could examine the validity of the identification of factors.

Factor 1 was characterized by a significant amount of ethane (57.57%), propane (36.27%), C5–C6 alkanes (24.64%–42.92%), acetylene (33.76%), and benzene (31.98%). Ethane and acetylene are connected with incomplete combustion, and C3–C6 alkanes are the main components of LPG and NG [40,41]. LPG and NG both play important role in vehicles, industrial process, and domestic catering. Influenced by new energy vehicles on the roads around, the concentrations of factor 1 were higher in the morning and evening than at noon in HP and ZH. The diurnal variations of factor 1 were steady in XS because of the stable petrochemical industry. Therefore, factor 1 was identified as LPG/NG usage including fuel combustion and evaporation in vehicles, industry, and households. Nowadays the fuel substitution from coal and oil to LPG and NG has been advanced rapidly in Hangzhou, making the NG/LPG more vital to ambient VOCs.

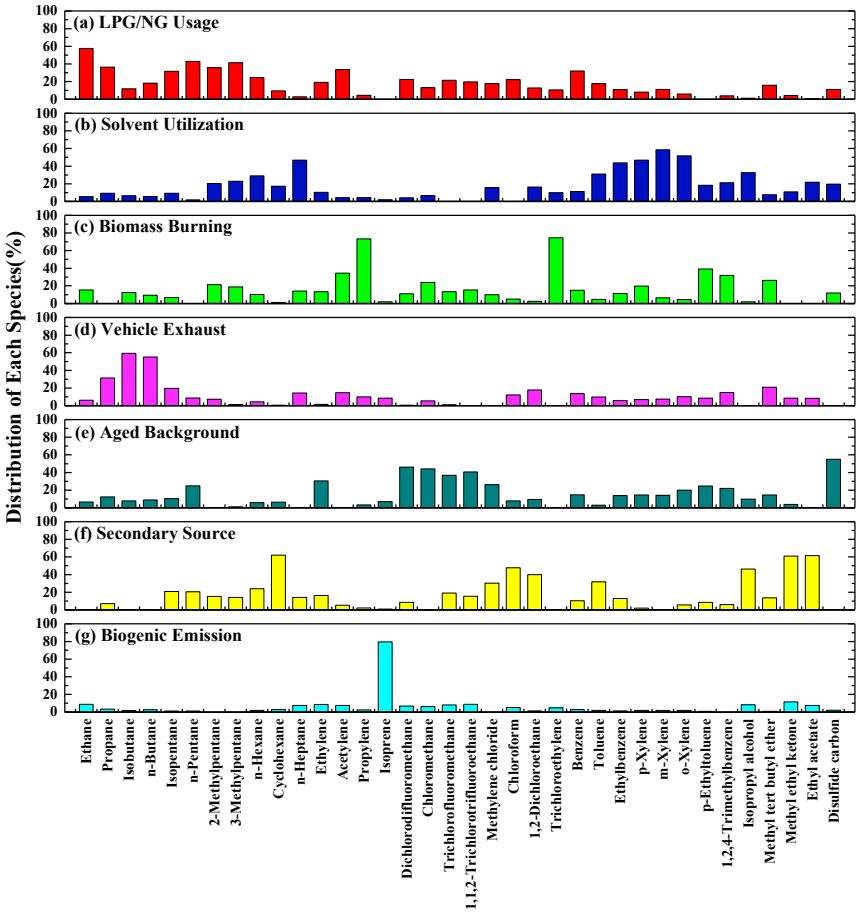


**Figure 5.** Explained variation of seven factors resolved with the Positive Matrix Factorization (PMF) model: (**a**) liquefied petroleum gas/natural gas (LPG/NG) usage, (**b**) solvent utilization, (**c**) biomass and burning, (**d**) vehicle exhaust, (**e**) aged background, (**f**) secondary source, (**g**) biogenic emission.

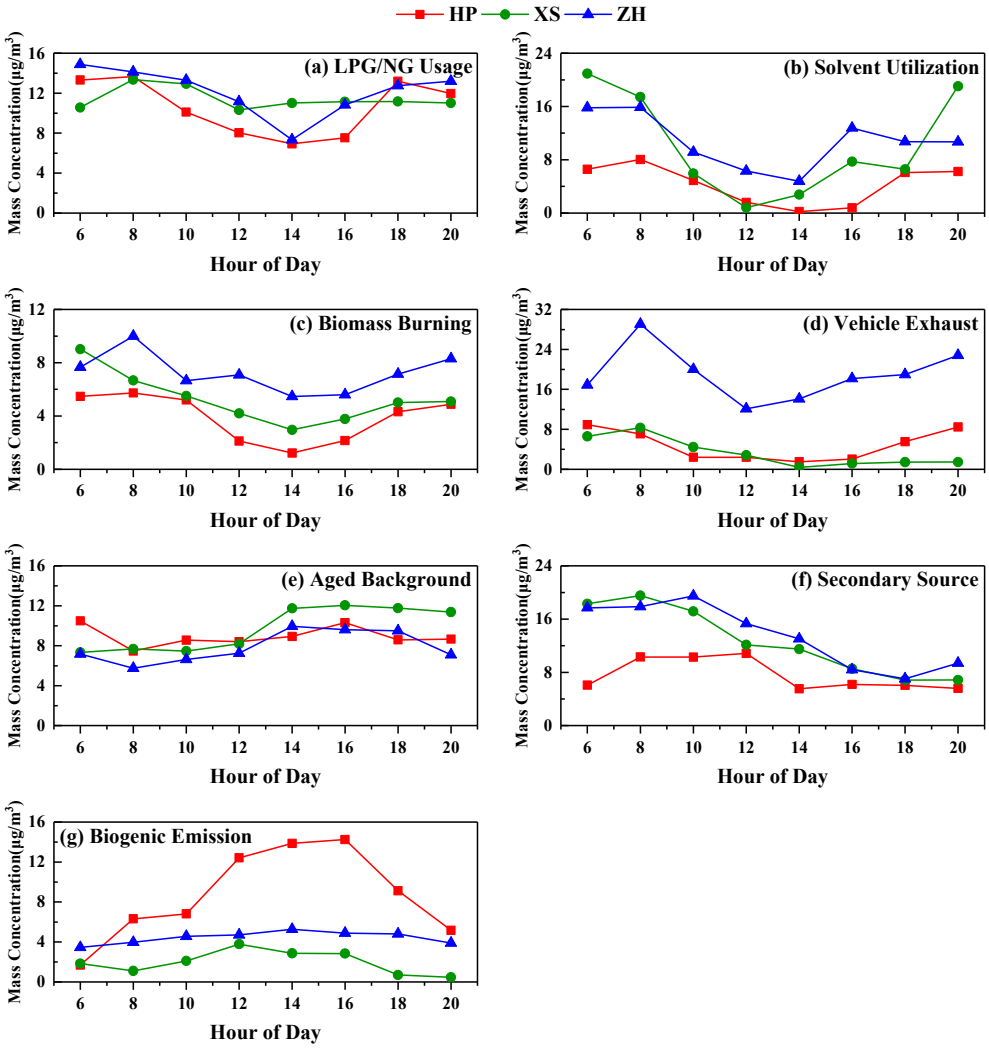


**Figure 6.** Diurnal variation of seven factors at the three sites: (**a**) liquefied petroleum gas/natural gas (LPG/NG) usage, (**b**) solvent utilization, (**c**) biomass and burning, (**d**) vehicle exhaust, (**e**) aged background, (**f**) secondary source, (**g**) biogenic emission.

Factor 2 was rich in n-hexane (28.90%), n-heptane (46.85%), BTEX (30.92%–51.68%), isopropyl alcohol (32.63%), and ethyl acetate (21.86%). It is known that BTEXs are the major constituents of solvents [42,43]. The amounts of aromatics are controlled strictly at present in China, thus some factories substitute OVOCs for BTEX in solvent use. For example, isopropyl alcohol and ethyl acetate are the common OVOCs solvents in industry [44,45]. n-Hexane and n-heptane are also widely used as nonpolar solvents in industrial processes [46]. Above all, factor 2 was named solvent utilization. From the point of daily variation, higher concentrations of solvent use were in XS and ZH, influenced by the surrounding industry and hospital, respectively.

High loading of propylene (73.26%) and trichloroethylene (74.58%) was found in factor 3. In addition, acetylene, chloromethane, p-ethyltoluene, and 1,2,4-trimethylbenzene occupied a high proportion as well. These compounds mainly come from chemical manufacturing and fuel combustion. Specifically propylene, acetylene, and chloromethane are the marker products of biomass combustion, and aromatics were also released during the biomass combustion [47,48]. Thus, factor 3 was recognized as biomass burning.

Factor 4 was distinguished by the dominant presence of C3–C5 alkanes (19.59%–59.49%), acetylene (14.74%), and methyl tert butyl ether (MTBE, 20.99%), which were typical tracers of vehicle emissions. Acetylene is the tracer of incomplete combustion, and MTBE is a widely used gasoline additive to raise the octane number [39]. The concentration displayed a bimodal diurnal profile in

ZH, much higher than HP and XS, which accorded with the effect of vehicle emissions on the three sites. Thus, factor 4 was considered to be vehicle exhaust.

Factor 5 explained high amounts of disulfide carbon (50.99%) and a series of halocarbons including dichlorodifluoromethane (46.13%), chloromethane (44.24%), 1,1,2-trichloro trifluoroethane (40.65%), and so on. These species are unreactive and have a long lifetime in the atmosphere [49]. The concentrations showed a small difference and steady variation at the three sites. Therefore, factor 5 was linked to aged background.

Factor 6 was associated with secondary generation, identified by OVOCs such as isopropyl alcohol (46.26%), methyl ethyl ketone (MEK, 60.89%), and ethyl acetate (61.54%), which mainly came from the photochemical reactions of NMHCs. The three sites showed the same variation: as sunlight intensity increased in the morning, primary pollutants accumulating in the evening were transformed into secondary pollutants. The concentration of factor 3 gradually decreased when the solar radiation reduced in the afternoon. Thus, factor 6 was identified as secondary source.

Factor 7 was almost solely dominated by isoprene (79.62%), which was the indicator of biogenic emissions, especially from broad-leafed trees [50,51]. The higher concentration in HP fitted the vegetation coverage at the three sites. The single-peak diurnal variation of factor 7 in HP also correlated well with temperature and solar radiation, consistent with biogenic emission.

Figure S4 compared the VOCs fraction between the measured source profiles and PMF factors of primary emission. The source profiles of solvent utilization, biomass burning, and vehicle exhaust were sampled in this study, and the source profile of LPG/NG usage was extracted from a previous paper [52]. The major species in the two profiles were almost overlapped, and the differences between them were within reasonable ranges. The above comparison results supported the accuracy of our PMF resolved factors, which improved our confidence for the source apportionment results.

### 3.2.2. Source Apportionment Results

Figure 7 presents the mass concentrations percentage of seven factors at the three sites. It should be noted that observed concentrations do not take into account the long-range transport and photochemical losses from emission sources to receptor sites. This likely results in an overestimation of relative contributions of some factors such as aged background and also an underestimation such as biogenic emission, but the comparison among the three sampling sites could still indicate the effect of emission sources on ambient air. In HP, biogenic emission accounted for 17.83%, much higher than in XS and ZH. Besides, LPG/NG usage, aged background, and secondary source contributed 21.70%, 18.29%, and 15.61% respectively, accounting for the major TVOC concentrations in HP. In XS, solvent utilization and secondary source contributed 18.65% and 23.13%, which were higher than in HP and ZH. LPG/NG usage and aged background also played important role, accounting for 21.00% and 17.81%. In ZH, vehicle exhaust source was the largest contributor, accounting for 25.34%, followed by secondary source (18.03%), LPG/NG usage (16.25%), and solvent utilization (14.34%). To sum up, LPG/NG usage, aged background, and secondary source were the major contributors to TVOCs in the whole of Hangzhou city.

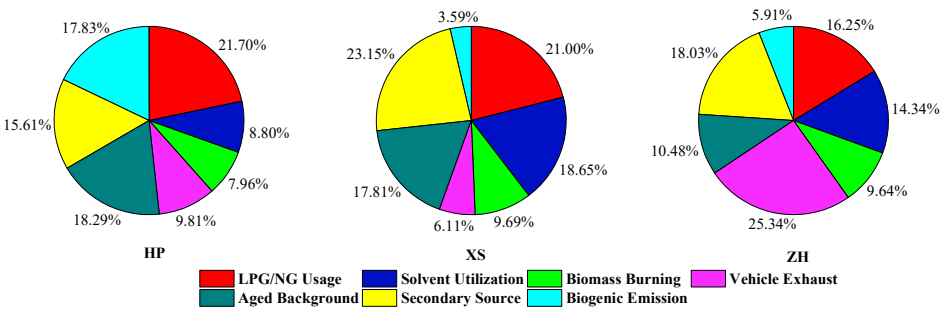


**Figure 7.** Relative contributions of seven sources to the ambient VOCs mass concentrations at the three sites.

### *3.3. The Roles of VOCs in $O_3$ Formation*

#### 3.3.1. VOCs Photochemical Reactivity

The reactivity is an important indicator that is usually used to estimate the ozone formation contribution for ambient VOCs. Table 1 lists the top 10 species based on Prop-E and ozone formation potential (OFP) at the three sampling sites. In terms of Prop-E, isoprene was dominant among all the sites, because of the high-activity with OH radicals. Regarding OFP, the highest species was isoprene in HP but ethylene in XS and ZH. There were more than 50% species overlapped among the three sites, representing the general ozone formation in Hangzhou. Based on these two indicators, isoprene, ethylene, m-xylene, toluene, and propylene were on the list in all sites, indicating that they were the most reactive species in Hangzhou.

Figure 8 classifies VOCs by functional groups and presents the calculated fractions of different groups based on volume mixing ratio (VMR), Prop-E, and OFP. Compared among the three sampling sites, concentrations of alkanes were higher in ZH because of the vehicle emissions, especially reactive high-carbon-number alkanes from diesel vehicles. The Prop-E and OFP of alkenes and alkynes were higher in HP than in XS and ZH, because isoprene was the most reactive species in 107 VOCs and almost from plants. By considering the three criteria, although alkanes, halocarbons, and OVOCs contributed 78%–82% VMR in total, they accounted for less than 34% Prop-E and OFP. However, alkenes and aromatics altogether contributed more than 65% Prop-E and OFP even with a small proportion of 20% VMR.

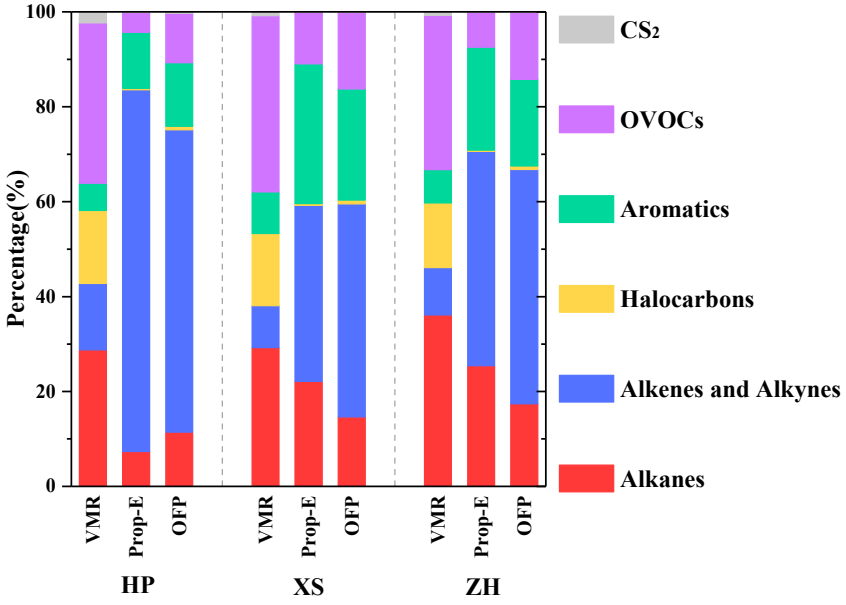


**Figure 8.** Percentage contributions of VOC group compositions to volume mixing ratio (VMR), propylene-equivalent concentrations (Prop-E), and ozone formation potential (OFP) at the three sites.

**Table 1.** Top 10 species based on propylene-equivalent concentrations (Prop-E) and ozone formation potential (OFP) at the three sites during sampling days.

| HP | | | | XS | | | | ZH | | | |
|---|---|---|---|---|---|---|---|---|---|---|---|
| **Compound** | **Prop-E (ppbC)** | **Compound** | **OFP (ppbv)** | **Compound** | **Prop-E (ppbC)** | **Compound** | **OFP (ppbv)** | **Compound** | **Prop-E (ppbC)** | **Compound** | **OFP (ppbv)** |
| Isoprene | 38.42 | Isoprene | 21.28 | Isoprene | 10.33 | Ethylene | 16.79 | Isoprene | 24.12 | Ethylene | 21.32 |
| m-Xylene | 1.35 | Ethylene | 15.26 | m-Xylene | 2.43 | Isoprene | 5.72 | n-Dodecane | 6.17 | Isoprene | 13.36 |
| Ethylene | 1.06 | Propylene | 3.37 | Toluene | 2.09 | Toluene | 5.56 | m-Xylene | 2.77 | Propylene | 8.21 |
| Toluene | 0.99 | Acetone | 2.74 | n-Undecane | 1.77 | Propylene | 4.43 | n-Undecane | 2.41 | Toluene | 4.88 |
| Propylene | 0.87 | Toluene | 2.65 | Styrene | 1.44 | m-Xylene | 3.34 | Propylene | 2.11 | Acetone | 3.89 |
| Vinyl acetate | 0.65 | m-Xylene | 1.85 | Ethylene | 1.17 | Acetone | 2.82 | Toluene | 1.83 | n-Butane | 3.87 |
| o-Xylene | 0.64 | n-Butane | 1.60 | Propylene | 1.14 | o-Xylene | 2.06 | Styrene | 1.67 | m-Xylene | 3.79 |
| 1,2,4-Trimethylbenzene | 0.63 | o-Xylene | 1.16 | o-Xylene | 1.13 | Methyl ethyl ketone | 1.55 | Vinyl acetate | 1.56 | Acrolein | 3.72 |
| n-Pentane | 0.61 | n-Pentane | 1.08 | Isopropyl alcohol | 1.08 | Acrolein | 1.55 | Naphthalene | 1.49 | Isobutane | 3.05 |
| Isopropyl alcohol | 0.59 | Methyl ethyl ketone | 1.05 | Vinyl acetate | 1.03 | n-Butane | 1.47 | Ethylene | 1.48 | 1-Butene | 2.45 |

3.3.2. Determination of $O_3$ Photochemical Regimes

SPM was used to assess the $O_3$ photochemical regimes based on the extent values $E(t)$. Explanations for SPM results are as following: the $O_3$ production is under a VOC-limited regime when $E(t)$ is less than 0.6 and NOx-limited regime when $E(t)$ is greater than 0.9. $O_3$ production is sensitive to both NOx and VOCs (transition regime) when $0.6 < E(t) < 0.9$ [53]. The time series of $E(t)$ and $O_3$ concentration are shown in Figure 9.

Comparing the three sites, $E(t)$ was generally higher in HP because of the abundance of biogenic emissions and lack of NOx anthropogenic pollution. Regarding the diurnal variation of $E(t)$, it was lower and the $O_3$ production tended to be under a VOC-limited regime in the morning. At about 10:00, $E(t)$ went up to 0.6 and the system turned into a transition regime. At 13:00–16:00, $E(t)$ reached the peak and the system was under a NOx-limited or transition regime. Then $E(t)$ declined with the arrival of evening rush hours. As shown in Figure 9, there was a strong relationship between $E(t)$ and $O_3$ concentration. Furthermore, the correlation analysis relating $E(t)$ with $O_3$ concentration is presented in Figure S5. It was found that there was an obvious positive correlation between the two variables, and the correlation coefficient was 0.77 in Hangzhou. The $O_3$ production was under a VOC-limited regime when $O_3$ concentration was below 110 μg/m$^3$, a NOx-limited regime when $O_3$ concentration was greater than 180 μg/m$^3$, and a transition regime when $O_3$ concentration was between 110 and 180 μg/m$^3$.

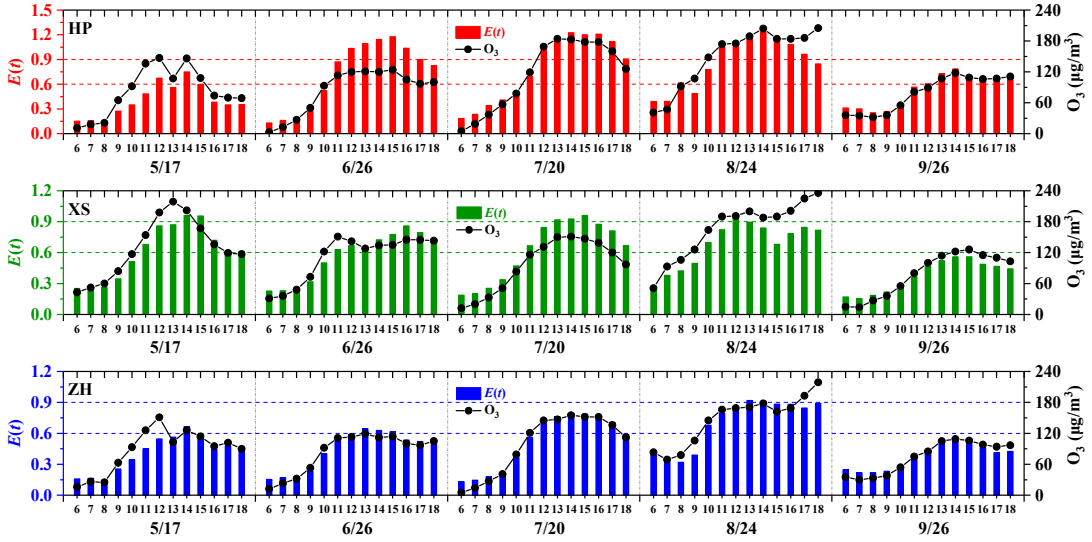


**Figure 9.** Time series of $E(t)$ and $O_3$ concentration at the three sites during sampling days.

## 4. Conclusions

An ambient VOCs sampling campaign was conducted at three sites (HP, XS, and ZH) in Hangzhou from May to September 2018, and 120 samples were obtained. The $O_3$ concentration in the downwind tended to be highest, while the concentrations of $NO_2$ and VOCs were lower in HP than XS and ZH. The average total VOC volume mixing ratios in HP, XS, and ZH were 32.00, 36.63, and 50.34 ppbv, respectively. Acetone was the most abundant compound at the three sites, accounting for about 20% among the 107 species. TVOCs, alkanes, and aromatics exhibited a steady distribution in HP, U-shaped in XS, and bimodal in ZH of diurnal variation. Propane and n-butane, tracers of vehicle exhaust, were much more abundant in ZH and exhibited bimodal profiles. Isoprene, an indicator of biogenic emissions, showed a unimodal distribution in HP. Chloromethane and 1,2-dichloroethane were unreactive species with relatively steady concentrations.

Seven factors were identified with PMF, consisting of LPG/NG usage, solvent utilization, biomass burning, vehicle exhaust, aged background, secondary source, and biogenic emission. The accuracy of results was examined by the diurnal variation of factors and the comparison between

measured source profiles and PMF factors. Biogenic emission in HP, solvent utilization in XS, and vehicle exhaust in ZH were much higher than the rest of the sites, contributing 17.83%, 18.65%, and 25.34%, respectively. In summary, the relative contributions of LPG/NG usage, aged background, and secondary source were 19.65%, 15.53%, and 18.93% in the whole of Hangzhou, which indicated the three sources were the major contributors to TVOCs.

Combining Prop-E with OFP, isoprene, ethylene, m-xylene, toluene, and propylene were identified as the most reactive species in Hangzhou, and alkenes and aromatics altogether contributed most Prop-E and OFP by 73.82% and 70.98%, with 18.13% of VMR. The SPM results indicated that $O_3$ formation was generally VOC-limited in the morning and evening, and a NOx-limited and transition regime at noon. There was an obvious positive correlation between $O_3$ concentration and $E(t)$, which helps to estimate the $O_3$ photochemical regimes by $O_3$ concentration.

**Supplementary Materials:** The following are available online at www.mdpi.com/xxx/s1.

**Author Contributions:** Conceptualization, L.H., K.L. and M.A.; Formal analysis, L.H., Y.Z. and X.Z.; Funding acquisition, L.C. and K.C.; Methodology, L.H., Y.Z. and X.Z.; Project administration, L.H. and Z.B.; Resources, L.C. and K.C.; Supervision, L.C.; Writing—original draft, L.H.; Writing—review and editing, L.C., K.L. and M.A.

**Funding:** This work was funded by the National Natural Science Foundation of China (No. 51876190), National Science Foundation of China (No. U1609212), National Key Research and Development Program of China (Grant No.2018YFB0605200), the Project of Hangzhou Technology (20162013A06), the Innovative Research Groups of the National Natural Foundation of China (No.51621005), and the program of Introducing Talents of Discipline to University (No.B08026).

**Acknowledgments:** We thank the Hangzhou Environmental Monitoring Center Station for providing the relevant meteorological pollutants data. We would like to thank the editors for modifying and revising this manuscript.

**Conflicts of Interest:** The authors declare no conflict of interest.

## References

1. Cheng, N.; Chen, Z.; Sun, F.; Sun, R.; Dong, X.; Xie, X.; Xu, C. Ground ozone concentrations over Beijing from 2004 to 2015: Variation patterns, indicative precursors and effects of emission-reduction. *Environ. Pollut.* **2018**, *237*, 262–274.
2. Li, L.; An, J.; Huang, L.; Yan, R.; Huang, C.; Yarwood, G. Ozone source apportionment over the Yangtze River Delta region, China: Investigation of regional transport, sectoral contributions and seasonal differences. *Atmos. Environ.* **2019**, *202*, 269–280.
3. Shen, J.; Zhang, Y.; Wang, X.; Li, J.; Chen, H.; Liu, R.; Zhong, L.; Jiang, M.; Yue, D.; Chen, D.; et al. An ozone episode over the Pearl River Delta in October 2008. *Atmos. Environ.* **2015**, *122*, 852–863.
4. Tan, Z.; Lu, K.; Jiang, M.; Su, R.; Dong, H.; Zeng, L.; Xie, S.; Tan, Q.; Zhang, Y. Exploring ozone pollution in Chengdu, southwestern China: A case study from radical chemistry to O3-VOC-NOx sensitivity. *Sci. Total Environ.* **2018**, *636*, 775–786.
5. Zeng, P.; Lyu, X.P.; Guo, H.; Cheng, H.R.; Jiang, F.; Pan, W.Z.; Wang, Z.W.; Liang, S.W.; Hu, Y.Q. Causes of ozone pollution in summer in Wuhan, Central China. *Environ. Pollut.* **2018**, *241*, 852–861.
6. Feng, Z.; Sun, J.; Wan, W.; Hu, E.; Calatayud, V. Evidence of widespread ozone-induced visible injury on plants in Beijing, China. *Environ. Pollut.* **2014**, *193*, 296–301.
7. Liu, H.; Liu, S.; Xue, B.; Lv, Z.; Meng, Z.; Yang, X.; Xue, T.; Yu, Q.; He, K. Ground-level ozone pollution and its health impacts in China. *Atmos. Environ.* **2018**, *173*, 223–230.
8. Li, L.; An, J.Y.; Shi, Y.Y.; Zhou, M.; Yan, R.S.; Huang, C.; Wang, H.L.; Lou, S.R.; Wang, Q.; Lu, Q.; et al. Source apportionment of surface ozone in the Yangtze River Delta, China in the summer of 2013. *Atmos. Environ.* **2016**, *144*, 194–207.
9. Jin, X.; Holloway, T. Spatial and temporal variability of ozone sensitivity over China observed from the Ozone Monitoring Instrument: Ozone Sensitivity over China. *J. Geophys. Res. Atmos.* **2015**, *120*, 7229–7246.
10. Gao, W.; Tie, X.; Xu, J.; Huang, R.; Mao, X.; Zhou, G.; Chang, L. Long-term trend of O3 in a mega City (Shanghai), China: Characteristics, causes, and interactions with precursors. *Sci. Total Environ.* **2017**, *603–604*, 425–433.

11. Wang, J.; Yang, Y.; Zhang, Y.; Niu, T.; Jiang, X.; Wang, Y.; Che, H. Influence of meteorological conditions on explosive increase in O3 concentration in troposphere. *Sci. Total Environ.* **2019**, *652*, 1228–1241.
12. Zhang, Z.; Zhang, X.; Gong, D.; Quan, W.; Zhao, X.; Ma, Z.; Kim, S. Evolution of surface O3 and PM2.5 concentrations and their relationships with meteorological conditions over the last decade in Beijing. *Atmos. Environ.* **2015**, *108*, 67–75.
13. Li, K.; Chen, L.; Fang, Y.; White, S.J.; Jang, C.; Wu, X.; Gao, X.; Hong, S.; Shen, J.; Azzi, M. Meteorological and chemical impacts on ozone formation: A case study in Hangzhou, China. *Atmos. Res.* **2017**, *196*, 40–52.
14. Paatero, P. Least squares formulation of robust non-negative factor analysis. *Chemom. Intell. Lab.* **1997**, *37*, 23–35.
15. Paatero, P.; Tapper, U. Positive matrix factorization: A non-negative factor model with optimal utilization of error estimates of data values. *Environmetrics* **2010**, *5*, 111–126.
16. Shao, P.; An, J.; Xin, J.; Wu, F.; Wang, J.; Ji, D.; Wang, Y. Source apportionment of VOCs and the contribution to photochemical ozone formation during summer in the typical industrial area in the Yangtze River Delta, China. *Atmos. Res.* **2016**, *176–177*, 64–74.
17. Wang, F.; Zhang, Z.; Acciai, C.; Zhong, Z.; Huang, Z.; Lonati, G. An integrated method for factor number selection of PMF model: Case study on source apportionment of ambient volatile organic compounds in Wuhan. *Atmosphere* **2018**, *9*, 390.
18. Liu, R.; Zhai, C.; Li, L.; Yu, J.; Liu, M.; Xu, L.; Feng, N. Concentration characteristics and source analysis of ambient VOCs in summer and autumn in the urban area of Chongqing. *Acta Sci. Circumstantiae* **2017**, *37*, 1260–1267.
19. Gong, X.; Hong, S.; Jaffe, D.A. Ozone in China: Spatial distribution and leading meteorological factors controlling O3 in 16 Chinese cities. *Aerosol Air Qual. Res.* **2018**, *18*, 2287–2300.
20. Li, B.; Ho, S.S.H.; Gong, S.; Ni, J.; Li, H.; Han, L.; Yang, Y.; Qi, Y.; Zhao, D. Characterization of VOCs and their related atmospheric processes in a central Chinese city during severe ozone pollution periods. *Atmos. Chem. Phys.* **2019**, *19*, 617–638.
21. EPA. *EPA Positive Matrix Factorization (PMF) 5.0 Fundamentals and User Guide*; United States Environmental Protection Agency: Washington, DC, USA, 2014.
22. Polissar, A.V.; Hopke, P.K.; Paatero, P.; Malm, W.C.; Sisler, J.F. Atmospheric aerosol over Alaska: 2. Elemental composition and sources. *J. Geophys. Res. Atmos.* **1998**, *103*, 19045–19057.
23. Chameides, W.L.; Fehsenfeld, F.; Rodgers, M.O.; Cardelino, C.; Martinez, J.; Parrish, D.; Lonneman, W.; Lawson, D.R.; Rasmussen, R.A.; Zimmerman, P. Ozone precursor relationships in the ambient atmosphere. *J. Geophys. Res. Atmos.* **1992**, *97*, 6037–6055.
24. Roger, A.; Janet, A. Atmospheric degradation of volatile organic compounds. *Chem. Rev.* **2003**, *103*, 4605.
25. Carter, W.P.L.; Pierce, J.A.; Luo, D.; Malkina, I.L. Environmental chamber study of maximum incremental reactivities of volatile organic compounds. *Atmos. Environ.* **1995**, *29*, 2513–2527.
26. Johnson, G.M. A simple model for predicting the ozone concentration of ambient air. In Proceedings of the Eighth International Clean Air Conference, Merrylands, Australia, 24 February 1984.
27. Blanchard, C.L.; Lurmann, F.W.; Roth, P.M.; Jeffries, H.E.; Korc, M. The use of ambient data to corroborate analyses of ozone control strategies. *Atmos. Environ.* **1999**, *33*, 369–381.
28. Wise, E.K. Climate-based sensitivity of air quality to climate change scenarios for the southwestern United States. *Int. J. Climatol.* **2009**, *29*, 87–97.
29. Karimov, K.A.; Gainutdinova, R.D. The long-term variations of ozone, UV-radiation and temperature in tropostratosphere and their connection with solar variability. In Proceedings of the SPIE 6733, International Conference on Lasers, Applications, and Technologies 2007: Environmental Monitoring and Ecological Applications, Minsk, Belarus, 9 July 2007.
30. Pang, X.; Mu, Y. Seasonal and diurnal variations of carbonyl compounds in Beijing ambient air. *Atmos. Environ.* **2006**, *40*, 6313–6320.
31. Lv, H.; Cai, Q.; Wen, S.; Chi, Y.; Guo, S.; Sheng, G.; Fu, J. Seasonal and diurnal variations of carbonyl compounds in the urban atmosphere of Guangzhou, China. *Sci. Total Environ.* **2010**, *408*, 3523–3529.
32. Weng, M.; Zhu, L.; Yang, K.; Chen, S. Levels and health risks of carbonyl compounds in selected public places in Hangzhou, China. *J. Hazard. Mater.* **2009**, *164*, 700–706.
33. Li, J.; Xie, S.D.; Zeng, L.M.; Li, L.Y.; Li, Y.Q.; Wu, R.R. Characterization of ambient volatile organic compounds and their sources in Beijing, before, during, and after Asia-Pacific Economic Cooperation China 2014. *Atmos. Chem. Phys.* **2015**, *15*, 7945–7959.

34. Cai, C.; Geng, F.; Tie, X.; Yu, Q.; An, J. Characteristics and source apportionment of VOCs measured in Shanghai, China. *Atmos. Environ.* **2010**, *44*, 5005–5014.
35. Liu, Y.; Shao, M.; Lu, S.; Chang, C.; Wang, J.; Chen, G. Volatile organic compound (VOC) measurements in the Pearl River Delta (PRD) region, China. *Atmos. Chem. Phys.* **2008**, *8*, 1531–1545.
36. Yang, Y.; Liu, X.; Zheng, J.; Tan, Q.; Feng, M.; Qu, Y.; An, J.; Cheng, N. Characteristics of one-year observation of VOCs, NOx, and O3 at an urban site in Wuhan, China. *J. Environ. Sci. China* **2019**, *79*, 297–310.
37. An, J.; Wang, Y.; Wu, F.; Zhu, B. Characterizations of volatile organic compounds during high ozone episodes in Beijing, China. *Environ. Monit. Assess.* **2012**, *184*, 1879–1889.
38. Chen, W.T.; Shao, M.; Lu, S.H.; Wang, M.; Zeng, L.M.; Yuan, B.; Liu, Y. Understanding primary and secondary sources of ambient carbonyl compounds in Beijing using the PMF model. *Atmos. Chem. Phys.* **2014**, *14*, 3047–3062.
39. Li, J.; Zhai, C.; Yu, J.; Liu, R.; Li, Y.; Zeng, L.; Xie, S. Spatiotemporal variations of ambient volatile organic compounds and their sources in Chongqing, a mountainous megacity in China. *Sci. Total Environ.* **2018**, *627*, 1442–1452.
40. Guo, H.; Zou, S.C.; Tsai, W.Y.; Chan, L.Y.; Blake, D.R. Emission characteristics of nonmethane hydrocarbons from private cars and taxis at different driving speeds in Hong Kong. *Atmos. Environ.* **2011**, *45*, 2711–2721.
41. Zheng, H.; Kong, S.; Xing, X.; Mao, Y.; Hu, T.; Ding, Y.; Li, G.; Liu, D.; Li, S.; Qi, S. Monitoring of volatile organic compounds (VOCs) from an oil and gas station in northwest China for 1 year. *Atmos. Chem. Phys.* **2018**, *18*, 4567–4595.
42. Yuan, B.; Shao, M.; Lu, S.; Wang, B. Source profiles of volatile organic compounds associated with solvent use in Beijing, China. *Atmos. Environ.* **2010**, *44*, 1919–1926.
43. Liao, K.; Hou, X. Optimization of multipollutant air quality management strategies: A case study for five cities in the United States. *J. Air Waste Manag. Assoc.* **2015**, *65*, 732–742.
44. Zheng, J.; Yu, Y.; Mo, Z.; Zhang, Z.; Wang, X.; Yin, S.; Peng, K.; Yang, Y.; Feng, X.; Cai, H. Industrial sector-based volatile organic compound (VOC) source profiles measured in manufacturing facilities in the Pearl River Delta, China. *Sci. Total Environ.* **2013**, *456–457*, 127–136.
45. Mo, Z.; Shao, M.; Lu, S. Review on volatile organic compounds (VOCs) source profiles measured in China. *Acta Sci. Circumstantiae* **2014**, *34*, 2179–2189.
46. Kwon, K.; Jo, W.; Lim, H.; Jeong, W. Characterization of emissions composition for selected household products available in Korea. *J. Hazard. Mater.* **2007**, *148*, 192–198.
47. Zhang, J.; Sun, Y.; Wu, F.; Sun, J.; Wang, Y. The characteristics, seasonal variation and source apportionment of VOCs at Gongga Mountain, China. *Atmos. Environ.* **2014**, *88*, 297–305.
48. Mo, Z.; Shao, M.; Lu, S. Compilation of a source profile database for hydrocarbon and OVOC emissions in China. *Atmos. Environ.* **2016**, *143*, 209–217.
49. McCarthy, M.C.; Hafner, H.R.; Chinkin, L.R.; Charrier, J.G. Temporal variability of selected air toxics in the United States. *Atmos. Environ.* **2007**, *41*, 7180–7194.
50. Fuchs, H.; Hofzumahaus, A.; Rohrer, F.; Bohn, B.; Brauers, T.; Dorn, H.; Häseler, R.; Holland, F.; Kaminski, M.; Li, X.; et al. Experimental evidence for efficient hydroxyl radical regeneration in isoprene oxidation. *Nat. Geosci.* **2013**, *6*, 1023.
51. Sindelarova, K.; Granier, C.; Bouarar, I.; Guenther, A.; Tilmes, S.; Stavrakou, T.; Müller, J.F.; Kuhn, U.; Stefani, P.; Knorr, W. Global data set of biogenic VOC emissions calculated by the MEGAN model over the last 30 years. *Atmos. Chem. Phys.* **2014**, *14*, 9317–9341.
52. Song, Y.; Dai, W.; Shao, M.; Liu, Y.; Lu, S.; Kuster, W.; Goldan, P. Comparison of receptor models for source apportionment of volatile organic compounds in Beijing, China. *Environ. Pollut.* **2008**, *156*, 174–183.
53. Blanchard, C.L.; Stoeckenius, T. Ozone response to precursor controls: Comparison of data analysis methods with the predictions of photochemical air quality simulation models. *Atmos. Environ.* **2001**, *35*, 1203–1215.